Available online at www.sciencedirect.com
ScienceDirect
Journal of Non-Crystalline Solids 353 (2007) 490–493
JOURNAL OF NON-CRYSTALLINE SOLIDS
www.elsevier.com/locate/jnoncrysol

Rare-earth doped photonic crystal microcavities prepared by sol–gel

Rui M. Almeida [a], Ana C. Marques [a,*], Alessandro Chiasera [b], Andrea Chiappini [c], Maurizio Ferrari [b]

[a] Departamento de Engenharia de Materiais/ICEMS, Instituto Superior Técnico/UTL Av. Rovisco Pais, 1049-001 Lisboa, Portugal
[b] IFN-CNR, Istituto di Fotonica e Nanotecnologie, CSMFO Group, via Sommarive 14, 38050 Povo-Trento, Italy
[c] Dipartimento di Fisica, Università di Trento, CSMFO Group, via Sommarive 14, 38050 Povo-Trento, Italy

Available online 7 February 2007

Abstract

Rare-earth doped photonic materials and structures have been prepared by sol–gel processing, in the form of 1D photonic bandgap multilayer stacks of silica and titania. A significant enhancement of the Er^{3+} emission at ca. 1530 nm occurred when these ions were inserted into Bragg mirrors and microcavities. In Er^{3+}/Yb^{3+} co-doped structures, an efficient energy transfer at 980 nm was observed from Yb^{3+} to Er^{3+} when these ions were in close proximity and especially when they were simultaneously present, in the same defect layer, with a 1530 nm photoluminescence enhancement of up to ~25 times being observed for excitation at 980 nm, compared to the excitation of the same microcavities samples at 514.5 nm.

PACS: 42.70.Qs; 77.55.+f; 81.20.Fw

Keywords: Photonic bandgap; Spin coating; Luminescence; Reflectivity; Silica; Rare-earths in glasses; Sol–gels (xerogels)

1. Introduction

Photonic bandgap (PBG) structures, also known as photonic crystals (PC's), are structures whose refractive index (or dielectric constant) is periodic on a length scale of the order of optical wavelengths (~100–1000 nm), which prevents light from propagating through the structures due to Bragg reflection [1]. A classical example of a PC in 1D is an interference filter (also called a Bragg mirror), which consists of a stack of alternating high and low refractive index dielectric layers of optical thickness (the physical thickness, x times the refractive index, n) equal to $\lambda/4$. Such a structure will exhibit a frequency region of high reflectivity, also called a 'stop band', where light undergoes Bragg reflection, with a maximum at the wavelength λ. Moreover, when the structure has a defect, such as one missing layer (equivalent to a double thickness layer of the other material), this will cause the occurrence of an allowed state localized inside the stop band, or 'pass band', which will increase the functionality of the 1D PBG structure. This particular example is called a Fabry–Perot microcavity [2–4], while the presence of two defects creates a coupled microcavity. In a Fabry–Perot microcavity, the reflectance minimum, corresponding to the microcavity resonance (or pass band), appears at $\lambda = 2nx$, where n and x are the refractive index and thickness of the defect layer. The quality factor (Q) of the microcavity is given by $Q = \lambda/\Delta\lambda$, where λ is the resonance wavelength and $\Delta\lambda$ is the resonance full width at half maximum (FWHM) [2]. Defects in microcavities can be doped with rare-earth elements like Er, which emits at the telecommunications operating wavelength of ca. 1530 nm. When the emitted light is resonant with the cavity, the Er^{3+} photoluminescence (PL) intensity should be enhanced by the factor Q [5]. Excitation can be provided with a diode laser at 980 nm, for example. However, the absorption cross-section of Er^{3+} is small at this

* Corresponding author. Tel.: +351 218418109; fax: +351 218418132.
E-mail address: ana.marques@ist.utl.pt (A.C. Marques).

0022-3093/$ - see front matter © 2007 Elsevier B.V. All rights reserved.
doi:10.1016/j.jnoncrysol.2006.10.015

wavelength, so that Yb^{3+} may be used as a co-dopant, to act as sensitizer [4,6–8]. Therefore, besides Er^{3+}-doped microcavities, Er^{3+}/Yb^{3+} co-doped structures have also been developed in this work, with the aims of increasing the Er^{3+} PL efficiency and studying the energy transfer process in the microcavity structures.

2. Experimental

Bragg mirrors (BM's) plus simple and coupled microcavities have been fabricated in the present work by sol–gel processing. The microcavities consisted of Er^{3+}-doped or Er^{3+}/Yb^{3+} co-doped active SiO_2 layers placed between BM's (also called distributed Bragg reflectors, or DBR's), each one consisting of three alternating SiO_2/TiO_2 pairs of layers. For the fabrication of multilayer stacks of silica and titania, the corresponding sols were first prepared. The preparation details, including the deposition on silica glass disks and the heat treatments performed, have been described in Ref. [4]. For the fabrication of the active layer, the SiO_2 sol was doped with Er (1 mol%) and/or Yb (2 mol%), in the form of nitrates. Thin films corresponding to the active layers only were also prepared (without Bragg mirrors) for comparison, using the same heat treatment in order to ensure similar levels of residual OH content (found, in a previous work [9], to be ca. 200 ppm for Er^{3+}/Yb^{3+} co-doped silicate films).

Angle-dependent reflectance spectra were obtained between 800 and 2500 nm, with a Nicolet 5700 FT-IR spectrometer (Thermo Electron Corporation), using unpolarized radiation. The Er^{3+} ($^4I_{13/2} \rightarrow {}^4I_{15/2}$) PL spectra were measured at room temperature, either in reflection mode, with the complementary excitation and detection angles (spectra of Figs. 3–5), or with detection perpendicular to the sample surface and excitation at 30° (spectra of Fig. 1). Further experimental details can also be found in Ref. [4].

3. Results

Er^{3+} PL measurements were performed on a BM with six doublets (SiO_2/TiO_2), including one Er^{3+}-doped silica layer in the middle and on a Er^{3+}-doped silica layer deposited on v-SiO_2 (F1). A significant intensification of the Er^{3+} PL at ~1530 nm in the active layer of the BM was found, compared to that obtained for the isolated doped film (F1). Fig. 1 shows an Er^{3+} PL emission at 1530 nm 17 times higher for the BM than for the corresponding isolated doped film (F1), with excitation at 514.5 nm and detection normal to the film. Note that both the active layer in the BM and film F1 had the same thickness ($\lambda/4n \sim 300$ nm) and the reflectance spectrum of such BM (spectrum not shown in this paper) shows a reflection band (stop band) laying between ~1100 and 2000 nm, for incidence at 10°.

Fig. 2 shows the angle-dependent reflectance spectra for a simple microcavity (designated by PBG_s), consisting of two 3-pair DBR's of alternating SiO_2 and TiO_2 layers, plus a sandwiched SiO_2 active defect layer doped with 1 mol% Er^{3+}. The cavity resonance wavelength, as well as the stop band centre, were tuned by varying the incidence angle (equal to the reflection angle). For 45° incidence, a stop band can be observed from about 1200 to 1900 nm with a maximum reflectance of 90%; a reflectance minimum appears at ca. 1530 nm, corresponding to the cavity resonance wavelength.

Fig. 3 shows the photoluminescence spectra of the simple microcavity described above for 514.5 nm excitation, at different detection angles, from 15° to 65°. The PL intensity presented a maximum for detection at 45° and it decreased as the angle of detection moved away from 45°. This

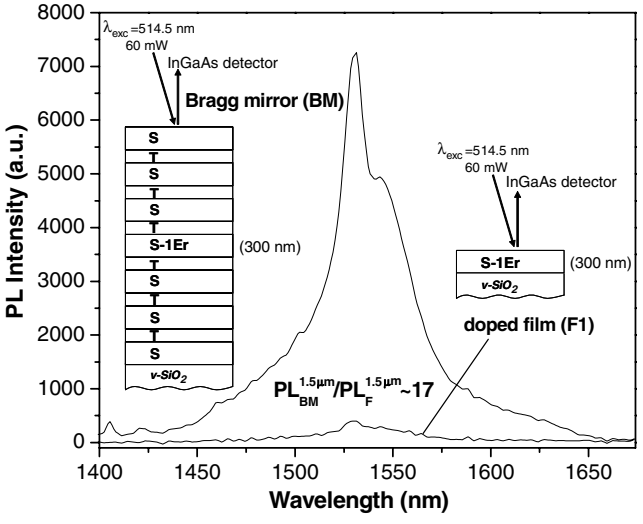

Fig. 1. Comparison between the Er^{3+} photoluminescence spectra of the active layer of a Bragg mirror and the corresponding doped film (F1). Both spectra were recorded in the same geometry, shown in the inset.

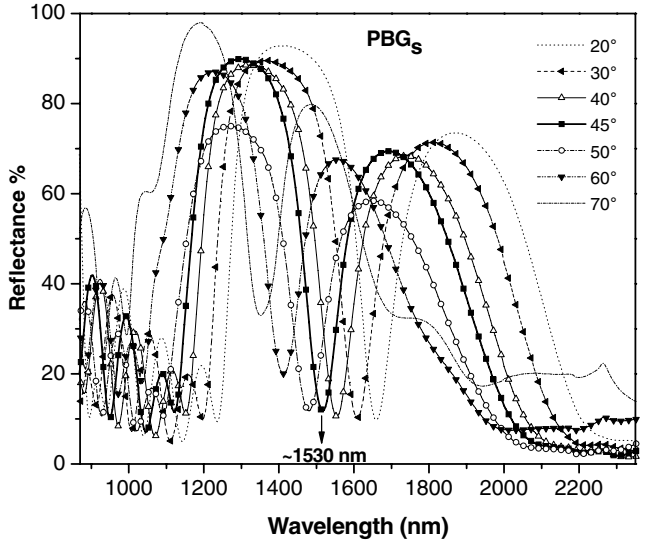

Fig. 2. Angle-dependent reflectance spectra of a simple Fabry–Perot microcavity, PBG_s, consisting of two 3-pair DBR's of alternating SiO_2 and TiO_2 layers, plus a sandwiched Er^{3+}-doped SiO_2 defect layer.

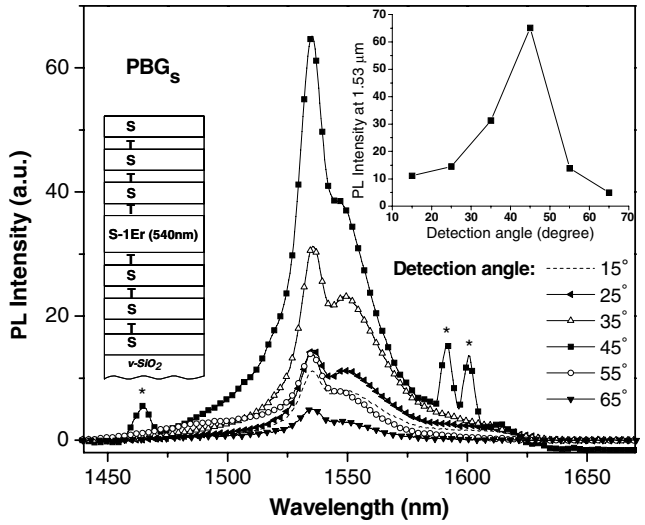

Fig. 3. Angle-dependent Er^{3+} PL spectra of PBG_s microcavity, obtained with 514.5 nm excitation. The schematic structure of the simple microcavity and the 1530 nm PL intensity versus detection angle are shown in the insets. Peaks marked with (*) were artifacts not related to the sample PL.

behavior can be followed in the inset of this figure. In addition, a change in the shape of the Er^{3+} PL spectra for different detection angles and, therefore, for different pass band wavelengths, is shown in Fig. 4.

The Er^{3+} PL spectra of a coupled microcavity, PBG_{C2}, with two Er^{3+}/Yb^{3+} co-doped SiO_2 defect layers, can be observed in Fig. 5, for excitations at 514.5 and 980 nm, respectively and detection at 10°. Note that the reflectance spectrum at 10° incidence for such structure exhibited a pass band centered at 1559 nm and $Q = 14$ (spectrum not shown in this paper). The Er^{3+} emission spectrum of the doped film (F2), composed of the two defect layers only (without DBR's) is also shown in Fig. 5 for comparison.

4. Discussion

Fig. 1 shows a strong enhancement of the Er^{3+} PL from the doped SiO_2 layer in a DBR, compared to the isolated doped film. This intensification occurred for the two excitation wavelengths tested, 514.5 nm (~17 times higher) and 980 nm (~11 times higher). At the origin of this phenomenon are the multiple reflections within the stacked (SiO_2/TiO_2) layers, as well as enhanced pumping by repeatedly reflected photons of 1530 nm wavelength, corresponding to a type of amplified spontaneous emission (ASE), a phenomenon which usually precedes laser oscillation.

In the angle-dependent reflectivity measurements shown in Fig. 2 for a simple microcavity (PBG_s), several interesting features may be noticed when the incidence angle increases (from 20° to 70°): (1) the pass band position shifts toward shorter wavelengths (blue shift), from 1660 to 1354 nm; (2) the stop band centre also has a blue shift; and (3) the stop band narrows, with its bandwidth decreasing from ~800 to ~520 nm. The blue shift of both the stop band (cen-

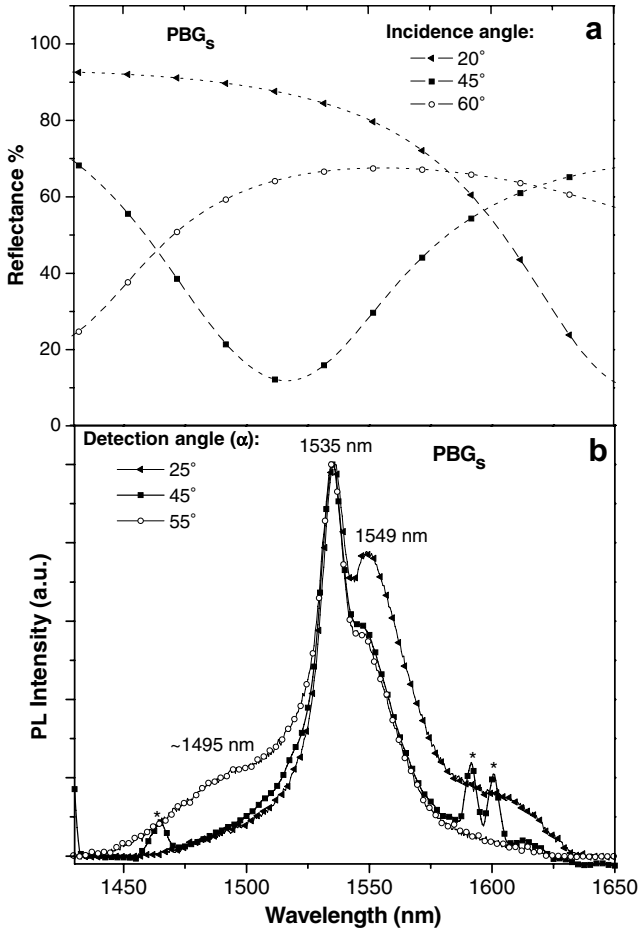

Fig. 4. (a) Angle-dependent reflectance spectra of PBG_s in the range of 1430–1650 nm (enlarged detail from Fig. 2). (b) Normalized Er^{3+} PL spectra of PBG_s as a function of the detection angle, for excitation at 514.5 nm, in the range of 1430–1650 nm. Peaks marked with (*) were artifacts not related to the sample PL.

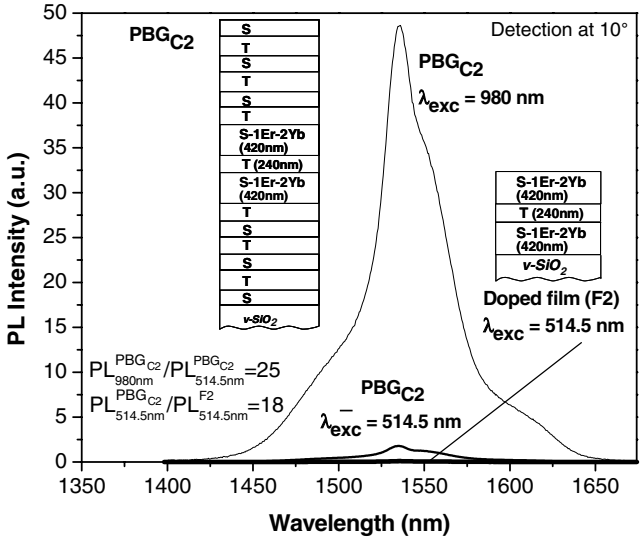

Fig. 5. Er^{3+} PL spectra of coupled microcavity, PBG_{C2}, for 514.5 nm and 980 nm excitation. The PL spectrum, taken with 514.5 nm excitation, for the corresponding doped film, F2, (without DBR's) is also shown for comparison. The insets show the schematic structures of PBG_{C2} and the doped film.

tre) and the defect (pass) band follows the modified form of Bragg's law [2]. The angle dependence of the pass band position is important, since it can be tailored to make the cavity resonant with the Er^{3+} emission wavelength at ~1530 nm. Fig. 2 shows the cavity resonance for PBG_s peaked at ca. 1530 nm for 45° incidence. This pass band presented a large FWHM of 110 nm (much larger than typical Er^{3+} PL 1530 nm peak width in a silica matrix) and a corresponding low Q value of ~14. The large value obtained for the width was mainly due to the limited number (only three) of SiO_2/TiO_2 pairs in each DBR. It is known that the number of pairs in each DBR, as well as a large refractive index contrast between each layer ($n(SiO_2) = 1.45$ and $n(TiO_2) = 2.00$) leads to a high DBR reflectivity and sharper pass bands, resulting in an increased quality factor or finesse of the cavity. For this reason (low Q), no significant narrowing of the Er^{3+}emission line at this wavelength could be observed for PBG_s (Figs. 3 and 4(b)). On the contrary, the PL spectra appear broader for detection angles far from 45° (see Fig. 4(b)), in particular for lower incidence angles (which correspond to pass band wavelengths longer than 1530 nm). For example, for detection at 25°, the PL FWHM was 37 nm, instead of the 25 nm obtained for 45° detection. The effect of a change in the Er^{3+} emission wavelength as a function of the detection angle, reported in other works [10,11], was not observed in this work, probably due to the low Q value and to a pass band much broader than the Er^{3+} PL spectrum. Nevertheless, the broadening of the Er^{3+} emission band for detection angles far from 45° may provide an interesting way to obtain a wider emission band for the Er^{3+} ions, since the typical value for a SiO_2 matrix is very low (ca. 8 nm [8]), even if the value obtained in this work in the absence of the broadening effect was larger than 8 nm (~25 nm, as in Fig. 4(b) for 45° detection). This may be of interest for wavelength division multiplexing (WDM) applications.

The inset of Fig. 3 clearly shows the Er^{3+} PL enhancement when the detection angle is 45°, the same angle which makes the cavity resonant with the typical Er^{3+} emission, at ~1530 nm (Fig. 4(a)). The ratio between the PL values measured for detection at 45° and 65° (where the pass band is totally non-resonant with 1530 nm) was ~13, a factor similar to the quality factor of PBG_s. Therefore, the presence of the cavity is shown to affect the Er^{3+} PL spectrum both in intensity and bandwidth.

The Er^{3+} PL measurements on Er^{3+}/Yb^{3+} co-doped cavities were made using two different excitation modes, in order to investigate the sensitizing or 'antenna' effect, consisting of Forster (non-radiative) energy transfer [12] from Yb^{3+} to Er^{3+} ions. Excitation with the 514.5 nm line promotes the $^4I_{15/2} \rightarrow {}^2H_{11/2}$ transition of Er^{3+}, whereas excitation with a diode laser at 980 nm (where the Er^{3+} absorption cross-section is ~3 times lower than at 514.5 nm) can induce energy transfer between Yb^{3+} and Er^{3+}, according to: $^2F_{5/2} + {}^4I_{15/2} \rightarrow {}^2F_{7/2} + {}^4I_{11/2}$. The microcavities fabricated in this work showed efficient energy transfer at 980 nm from Yb^{3+} to Er^{3+} ions, which can be observed in Fig. 5, where the PL spectrum recorded for PBG_{C2} (coupled microcavity with two defect layers co-doped with Er^{3+}/Yb^{3+}) was ~25 times more intense when excited at 980 nm than when excited at 514.5 nm. For pumping at 514.5 nm, when there is no Yb^{3+} sensitizing effect, the intensity of the Er^{3+} emission from the coupled microcavity, was found to be ~18 times stronger than that of the corresponding isolated film (F2). This enhancement can basically be attributed to the presence of the microcavity.

5. Conclusions

One-dimensional simple and coupled microcavities have been prepared by sol–gel processing, using silica and titania (anatase) alternating layers as the low and high refractive index materials, respectively. Enhancement of the Er^{3+} spontaneous PL emission was achieved when inserted into Bragg mirrors (by a factor of up to ~17) and microcavities (by a factor of up to ~18), compared to the corresponding isolated doped films. Angle-dependent microcavity resonance and Er^{3+} PL spectrum intensity and shape variations were found for the microcavities prepared. Er^{3+}/Yb^{3+} co-doped microcavities have been fabricated with the aim of increasing the Er^{3+} PL pumping efficiency, by energy transfer at 980 nm from Yb^{3+} to Er^{3+}. A strong sensitizing ('antenna') effect was observed when exciting Er^{3+} with 980 nm light in the presence of Yb^{3+}, if the two types of ions were in close proximity (sensitizing factor ~25).

Acknowledgements

This work was partially supported by a collaborative GRICES-CNR grant for the period of 2005/2006 and by MIUR-FIRB (RBNE012N3X-005).

References

[1] V. Berger, Curr. Opin. Solid State Mater. Sci. 4 (1999) 209.
[2] R.M. Almeida, Z. Wang, Proc. SPIE 4655 (2002).
[3] J. Belessa, S. Rabaste, J.C. Plenet, J. Dumas, J. Mugnier, O. Marty, Appl. Phys. Lett. 79 (2001) 2142.
[4] R.M. Almeida, A.C. Marques, J. Non-Cryst. Solids 352 (2006) 475.
[5] D. Kleppner, Phys. Rev. Lett. 47 (1981) 233.
[6] R. Wu, J.D. Myers, M.J. Myers, C. Rapp, Proc. SPIE 4968 (2003) 11.
[7] R.M. Almeida, A.C. Marques, S. Portal, Opt. Mater. 27 (2005) 1718.
[8] W.J. Miniscalco, in: M.J.F. Digonnet (Ed.), Rare-earth Doped Fiber Lasers and Amplifiers, Marcel Dekker, New York, 1993 (chapter 2).
[9] R.M. Almeida, X.M. Du, D. Barbier, X. Orignac, J. Sol–Gel Sci. Technol. 14 (1999) 209.
[10] E.F. Schubert, A. Vredenberg, N.E.J. Hunt, Y.H. Wong, P.C. Becker, J.M. Poate, D. Jacobson, L.C. Feldman, G.J. Zydzik, Appl. Phys. Lett. 61 (1992) 1381.
[11] A. Vredenberg, N.E.J. Hunt, E.F. Schubert, D.C. Jacobson, J.M. Poate, G.J. Zydzik, Phys. Rev. Lett. 71 (1993) 517.
[12] M.J.A. de Dood, J. Knoester, A. Tip, A. Polman, Phys. Rev. B 71 (2005) 115102.